

ADVANCED ENERGY MATERIALS

Supporting Information

for *Adv. Energy Mater.*, DOI: 10.1002/aenm.202000335

Correlating Macro and Atomic Structure with Elastic
Properties and Ionic Transport of Glassy $\text{Li}_2\text{S-P}_2\text{S}_5$ (LPS)
Solid Electrolyte for Solid-State Li Metal Batteries

*Regina Garcia-Mendez, Jeffrey G. Smith, Joerg C. Neuefeind,
Donald J. Siegel, and Jeff Sakamoto**

Supporting Information

Correlating macro and atomic structure with elastic properties and ionic transport of glassy $\text{Li}_2\text{S-P}_2\text{S}_5$ (LPS) solid electrolyte for solid-state Li metal batteries

Regina Garcia-Mendez, Jeffrey G. Smith, Joerg C. Neufeind, Donald J. Siegel and Jeff Sakamoto*

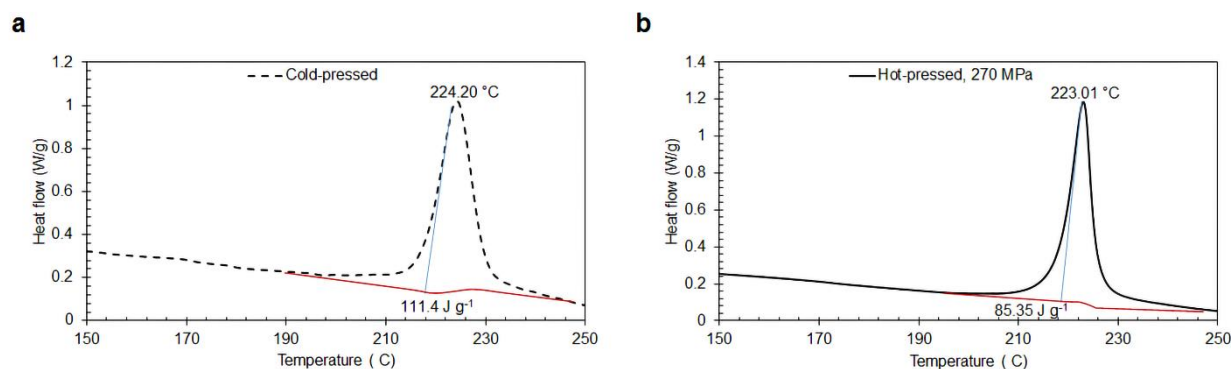


Figure S1. LPS 75-25 latent heat of crystallization of a (a) cold-pressed sample (b) hot-pressed sample at 270 MPa 200°C

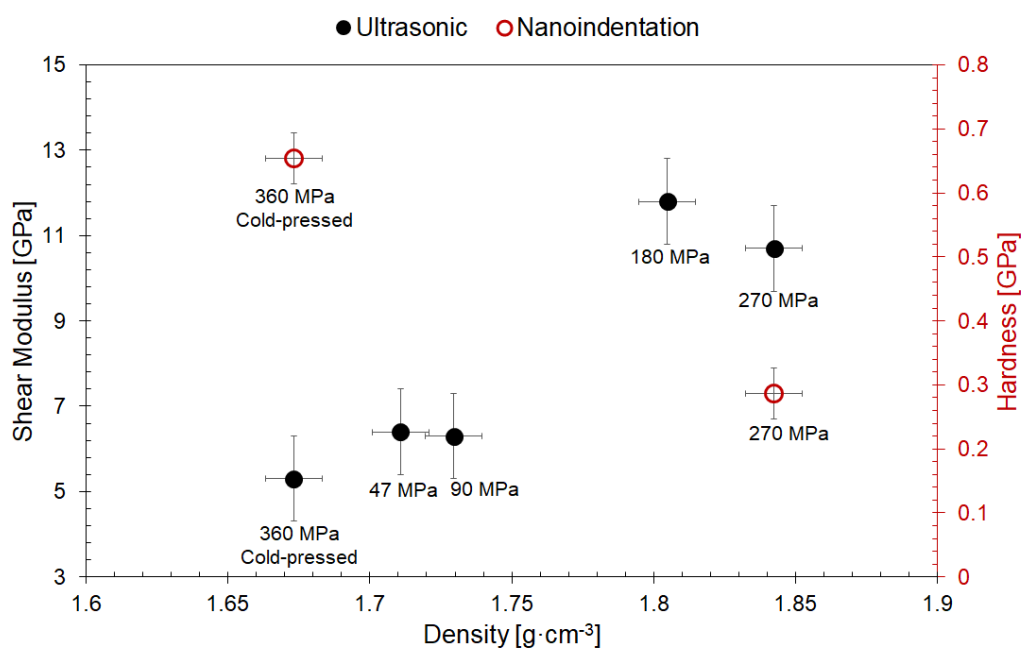


Figure S2. Shear Moduli of LPS 75-25 as a function of molding pressure via ultrasonic velocity measurements and Hardness values measured via nanoindentation

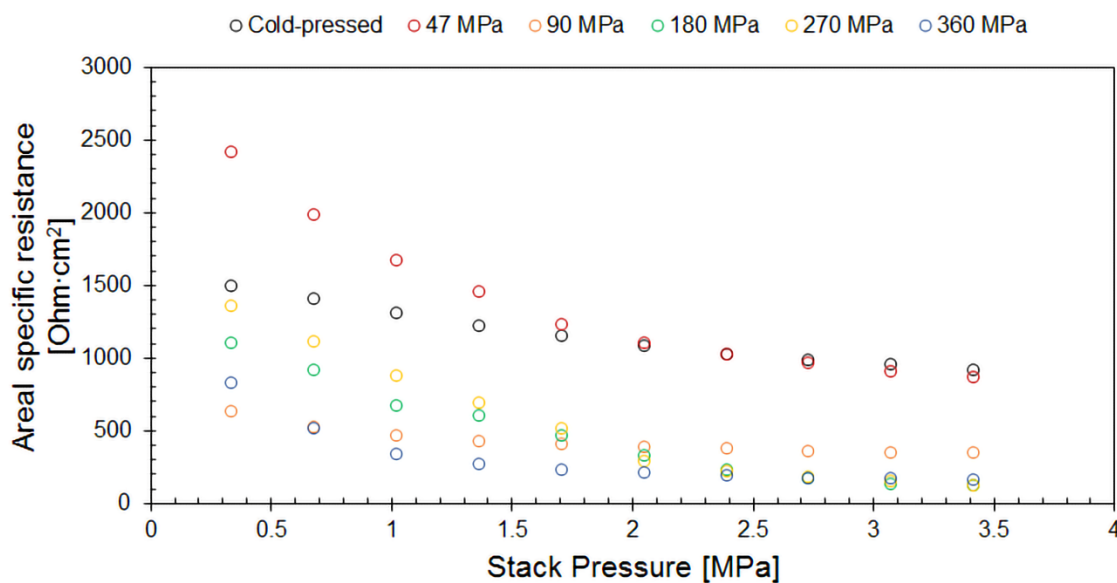


Figure S3. Effect of cell stack pressure on areal specific resistance for the bulk contribution in LPS 75-25 at room temperature

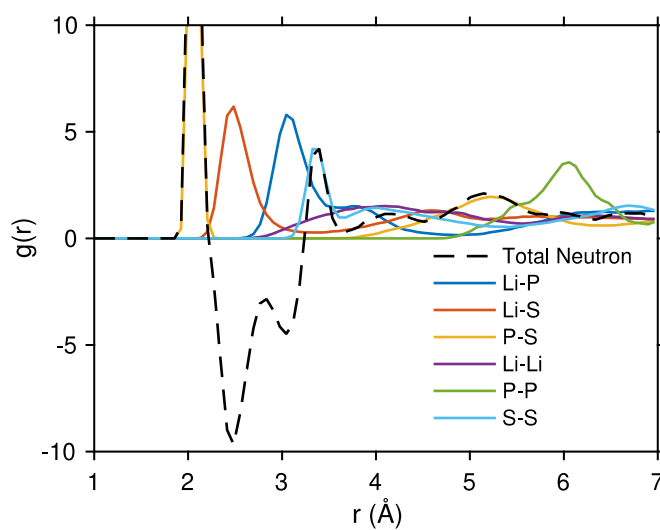


Figure S4. Local ordering of amorphous LPS 75-25 at 25 °C. Calculated partial pair distribution functions (p-PDF) and total neutron weighted PDF, $G'(r)$

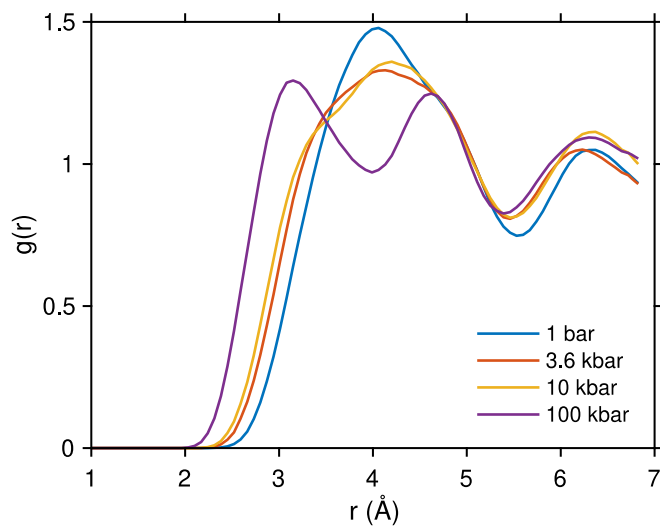


Figure S5. Calculated partial pair distribution function of Li-Li in LPS 75-25 at 25 °C for 1 bar, 3.6, 10, and 100 kbar.

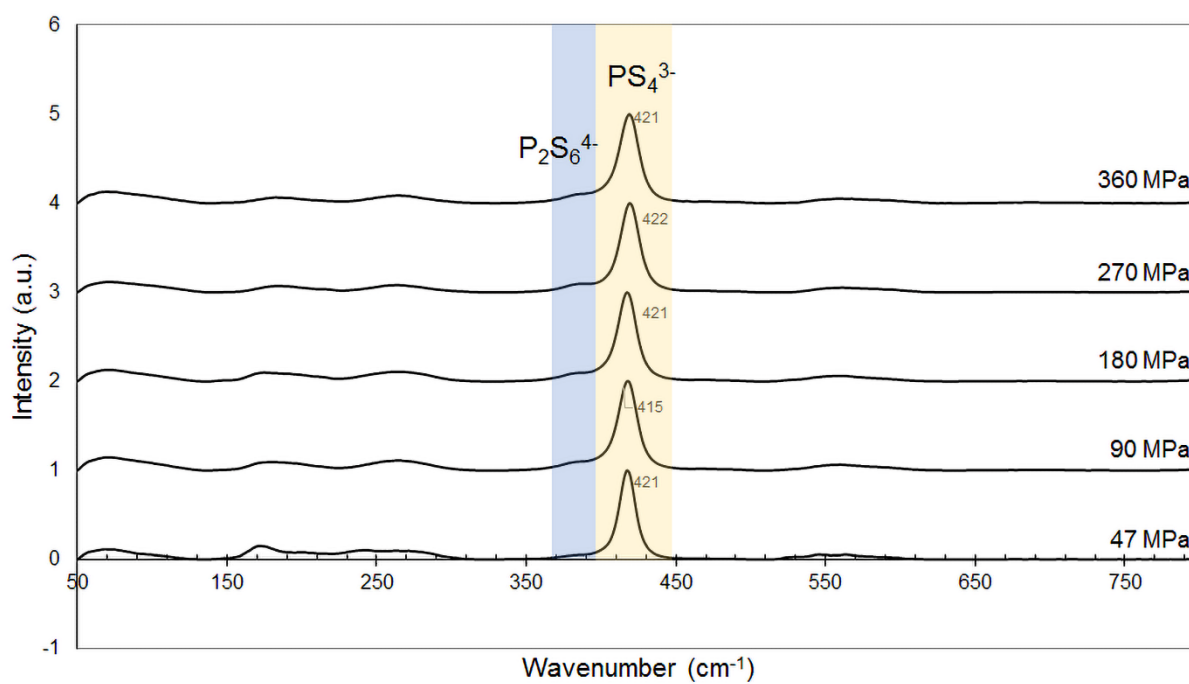


Figure S6. Raman spectra on LPS 75-25 samples processed at different molding pressures

Temperature [K]					
Density [g · cm ⁻³]	300	700	850	1000	E _a [eV]
1.56	7.08 x 10 ⁻⁸	1.99 x 10 ⁻⁵	4.04 x 10 ⁻⁵	7.08 x 10 ⁻⁵	0.255
1.65	7.80 x 10 ⁻⁸	1.94 x 10 ⁻⁵	4.58 x 10 ⁻⁵	6.70 x 10 ⁻⁵	0.251
1.76	9.64 x 10 ⁻⁸	1.91 x 10 ⁻⁵	3.45 x 10 ⁻⁵	6.34 x 10 ⁻⁵	0.238
1.89	6.47 x 10 ⁻⁸	1.55 x 10 ⁻⁵	3.23 x 10 ⁻⁵	5.32 x 10 ⁻⁵	0.248
2.42	9.60 x 10 ⁻¹⁰	2.01 x 10 ⁻⁶	5.09 x 10 ⁻⁶	1.13 x 10 ⁻⁵	0.345

Table S1. Calculated Li diffusion coefficients in cm²·s⁻¹ and energy of activation for ionic conduction in LPS 75-25 samples as a function temperature and pressure

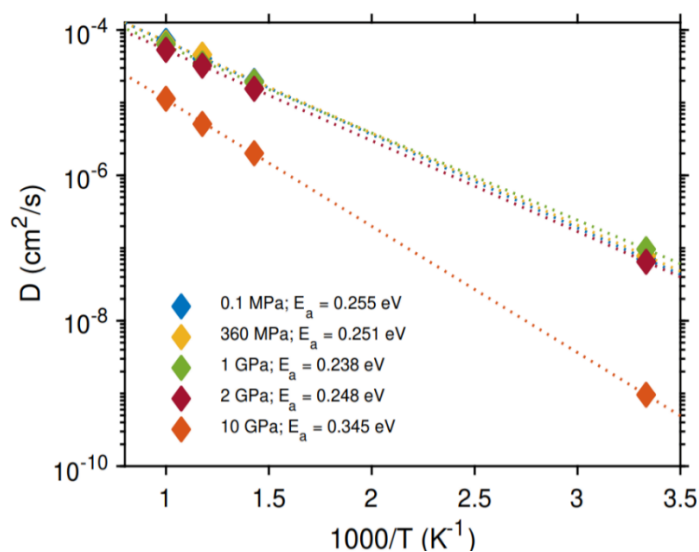


Figure S7. Calculated Arrhenius plot of Li diffusion coefficients and activation energies for LPS 75-25. Coefficients at room temperature are extrapolated from a linear fit (dotted lines) of the high temperature data.

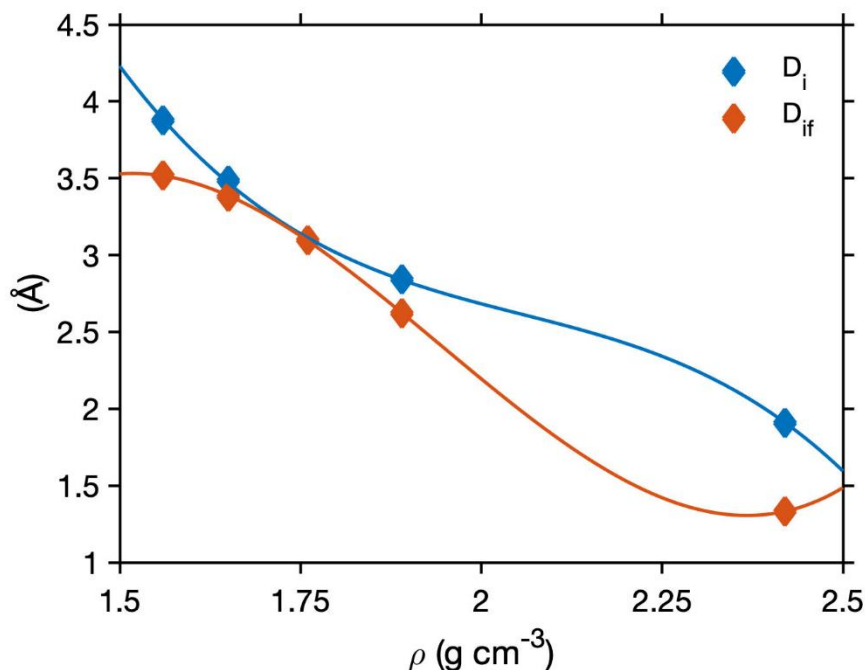


Figure S8. Calculated largest included sphere D_i (blue diamonds) and the largest included sphere along the free sphere path D_{if} (orange diamonds) in Li_3PS_4 glass. The lines are a cubic polynomial fit to the data at five densities.

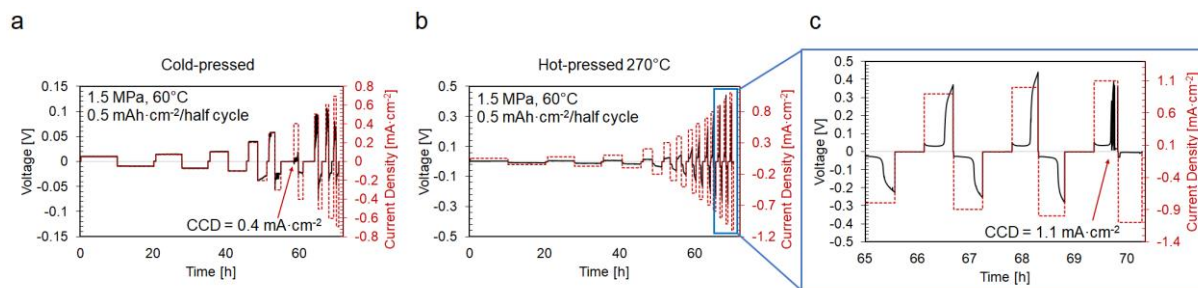


Figure S9. Critical Current Density (CCD) measurements of LPS 75-25 at 1.5 MPa, 60 °C. (a) Cold-pressed sample, (b) Hot-pressed sample at 270 MPa, (c) zoomed-in galvanostatic test of the hot-pressed sample at 270 MPa from 65 h to 72 h.

Stack pressure [MPa]	CCD [$\text{mA}\cdot\text{cm}^{-2}$]
1.5	0.3
3.1	0.4
6.2	0.4

Table S1. Critical Current Density (CCD) measurements of cold-pressed LPS 75-25 at room temperature, as a function of stack pressure

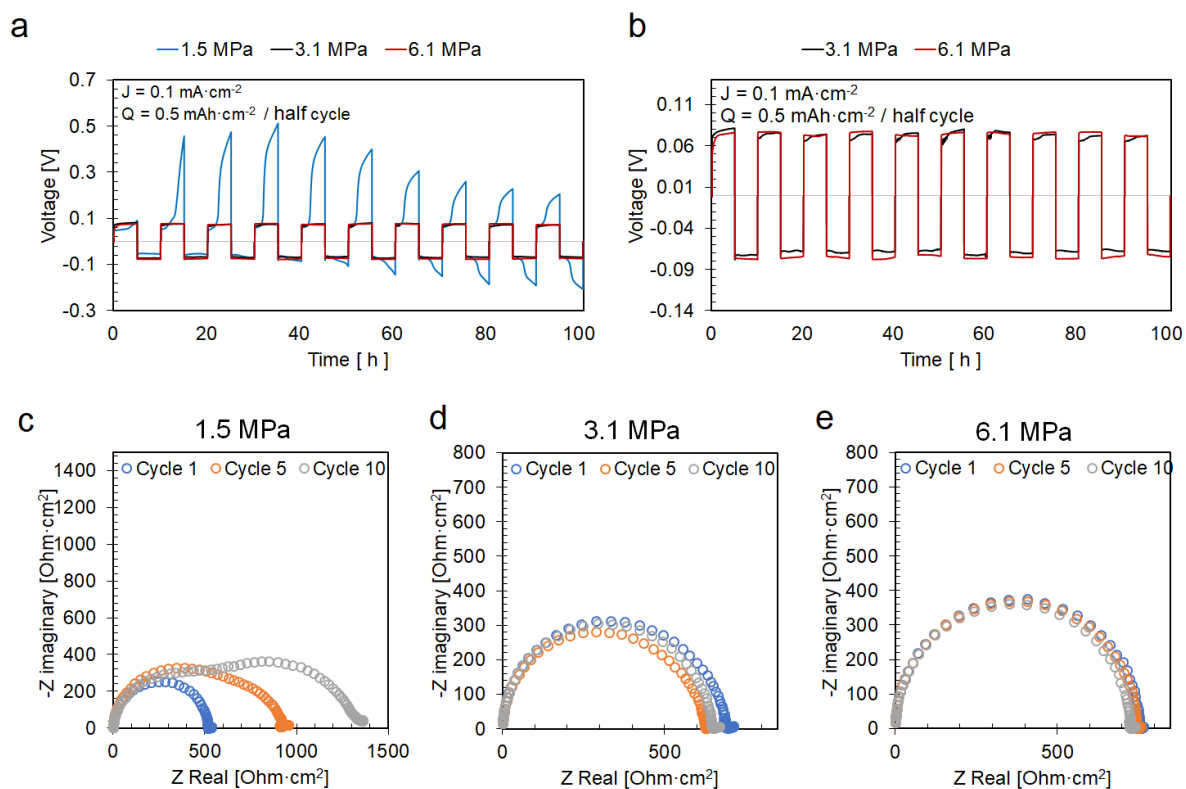


Figure S10. AC and DC testing of Li-LPS-Li symmetric cells under constant current density of $0.1 \text{ mA}\cdot\text{cm}^{-2}$, fixed charge of $0.5 \text{ mAh}\cdot\text{cm}^{-2}$ per half cycle as a function of stack pressure. (a) Voltage response as a function of stack pressure. (b) Voltage response under a stack pressure of 3.1 and 6.1 MPa. Impedance evolution at (c) 1.5 MPa, (d) 3.1 MPa, and (e) 6.1 MPa.